Journal of Experimental Botany, Vol. 64, No. 2, pp. 585–597, 2013
doi:10.1093/jxb/ers351 Advance Access publication 1 December, 2012
This paper is available online free of all access charges (see http://jxb.oxfordjournals.org/open_access.html for further details)

Journal of Experimental Botany
www.jxb.oxfordjournals.org

RESEARCH PAPER

AtFH1 formin mutation affects actin filament and microtubule dynamics in *Arabidopsis thaliana*

Amparo Rosero[1], Viktor Žárský[1,2] and Fatima Cvrčková[1,*]

[1] Department of Experimental Plant Biology, Faculty of Sciences, Charles University, Viničná 5, CZ 128 44 Praha 2, Czech Republic
[2] Institute of Experimental Botany, Academy of Sciences of the Czech Republic, Rozvojová 135, CZ 160 00 Prague 6, Czech Republic

* To whom correspondence should be addressed. E-mail: fatima.cvrckova@natur.cuni.cz

Received 30 April 2012; Revised 8 November 2012; Accepted 9 November 2012

Abstract

Plant cell growth and morphogenesis depend on remodelling of both actin and microtubule cytoskeletons. AtFH1 (At5g25500), the main housekeeping *Arabidopsis* formin, is targeted to membranes and known to nucleate and bundle actin. The effect of mutations in AtFH1 on root development and cytoskeletal dynamics was examined. Consistent with primarily actin-related formin function, *fh1* mutants showed increased sensitivity to the actin polymerization inhibitor latrunculin B (LatB). LatB-treated mutants had thicker, shorter roots than wild-type plants. Reduced cell elongation and morphological abnormalities were observed in both trichoblasts and atrichoblasts. Fluorescently tagged cytoskeletal markers were used to follow cytoskeletal dynamics in wild-type and mutant plants using confocal microscopy and VAEM (variable-angle epifluorescence microscopy). Mutants exhibited more abundant but less dynamic F-actin bundles and more dynamic microtubules than wild-type seedlings. Treatment of wild-type seedlings with a formin inhibitor, SMIFH2, mimicked the root growth and cell expansion phenotypes and cytoskeletal structure alterations observed in *fh1* mutants. The results suggest that besides direct effects on actin organization, the *in vivo* role of AtFH1 also includes modulation of microtubule dynamics, possibly mediated by actin–microtubule cross-talk.

Key words: Actin, *Arabidopsis*, At5g25500, LatB, microtubules, SMIFH2, VAEM.

Introduction

Plant growth, development, and morphogenesis are intimately associated with the dynamics of both microtubule and actin microfilament cytoskeletons (see, for example, Smith and Oppenheimer, 2005). Plant cell morphogenesis depends on mechanical properties of the cell wall, determined by organization of the cellulose microfibrils, interlinked with cortical microtubules (Emons *et al.*, 2007). Microfilaments contribute less directly, for example via participation in membrane recycling (Bannigan and Baskin, 2005), though they are important in tip-growing cells such as root hairs (Peremyslov *et al.*, 2010).

Root growth results from regulated cell divisions in the meristem, and anisotropic cell expansion and differentation in the elongation and differentiation zones. Mutations affecting the cytoskeleton often affect root growth or root hair development (Thitamadee *et al.*, 2002; Gilliland *et al.*, 2003; Abe and Hashimoto, 2005).

Formins (FH2 proteins) are key eukaryotic cytoskeletal regulators. Their hallmark FH2 domain can dimerize and nucleate actin (Blanchoin and Staiger, 2010). Seed plants have two formin clades with numerous paralogues (Deeks *et al.*, 2002; Grunt *et al.*, 2008); *in vitro* studies of several proteins demonstrated microfilament nucleation, capping, and binding (e.g. Ingouff *et al.*, 2005; Yi *et al.*, 2005). Metazoan formins also participate in remodelling the microtubular cytoskeleton (Bartolini and Gundersen, 2010). Similar observations were also reported for plant formins—*Arabidopsis* AtFH4 and AtFH14 (Deeks *et al.*, 2010; Li *et al.*, 2010) and rice FH5 (Yang *et al.*, 2011; Zhang *et al.*, 2011), which interact with microtubules using diverse mechanisms (see also Wang *et al.*, 2012).

AtFH4 is a class I formin, exhibiting the clade-specific structure with a signal peptide, a proline-rich extracellular domain, and a transmembrane domain in front of the conserved FH1 and FH2 domains (Cvrčková, 2000). It binds microtubules via a motif shared by a subgroup of class I formins, the GOE domain (Deeks *et al.,* 2010). AtFH14 and rice FH5 are typical class II formins with a PTEN-related domain in front of FH1 and FH2 (Grunt *et al.,* 2008); since they lack the GOE motif, they obviously bind microtubules by other means.

AtFH1 is the main housekeeping class I formin in *Arabidopsis thaliana*, as judged from its gene expression pattern (Zimmermann *et al.,* 2004). It has the typical class I structure, associates with membranes (Banno and Chua, 2000; Cheung and Wu, 2004), and its extracellular domain may anchor the actin cytoskeleton across the plasmalemma into the cell wall (Martiniere *et al.,* 2011). AtFH1 can nucleate and bundle actin (Michelot *et al.,* 2005, 2006); it contains no known microtubule-binding motifs, and no discernible phenotype was described so far in mutants lacking AtFH1, although its transient overexpression caused loss of pollen tube polarity (Cheung and Wu, 2004).

Here the characterization of seedling root development in mutants harbouring T-DNA insertions in the *AtFH1* locus is reported. While under normal conditions mutants exhibited no obvious phenotypic alterations, they were hypersensitive towards an anti-actin drug (alone or together with a microtubule inhibitor). Organization of microfilaments and microtubules in the mutant root cortex, as well as their dynamics, documented by variable-angle epifluorescence microscopy (VAEM; see Wan *et al.,* 2011), differed from those of wild-type (wt) plants. The growth and cytoskeletal organization phenotypes were mimicked by treatment with a specific inhibitor of FH2 domain function (Rizvi *et al.,* 2009). Thus, AtFH1 appears to participate in regulation of cytoskeletal dynamics *in vivo* by a mechanism involving cross-talk between actin and microtubules.

Materials and methods

Plants

Two T-DNA insertional mutants (*fh1-1*, SALK-032981; and *fh1-2*, SALK-009693) in the *AtFH1* gene (At5g25500) were obtained from the SALK Institute (Alonso *et al.,* 2003). To determine *AtFH1* allelic status, PCR using primers *fh1-1*-LP (5'GTCTCCGTCACTGTCGTTAGC3') with *fh1-1*-RP (5'TTGTTGTTTAACGACTTCGCC3') was employed to detect the wt allele in crosses involving *fh1-1*, and *fh1-2*-LP (5'TG TTTGTGTAGGCTGCTTGTG3') with *fh1-2*-RP (5'ATTCTTTCGTG GTACACACGG3') for the wt allele in crosses of *fh1-2*. For mutant alleles, the RP primers were combined with the SALK primer LBb1.3: 5'ATTTTGCCGATTTCGGAAC3' for the T-DNA insertion.

Mutants were crossed with green fluorescent protein (GFP)–MAP4 and GFP–FABD reporter lines (Marc *et al.,* 1998; Ketelaar *et al.,* 2004) as described (Cole *et al.,* 2005). Media with kanamycin and BASTA® were used to select GFP–MAP4- and GFP–FABD-carrying plants, respectively, and fluorescence was evaluated microscopically. Genotyping to select *fh1* homozygotes was done in the second and third generation.

RT–PCR

RNA was isolated from 7-day-old seedlings using the RNeasy Plant kit (Qiagen). First-strand cDNA synthesis and semi-quantitative reverse transcription–PCR (RT–PCR; with β-actin-specific primers for control) were performed according to Dvořáková *et al*. (2007) using 30 cycles, DreamTaq polymerase (Fermentas), and AtFH1-specific primers (5'GGATCCAGAAGAAAGAAGAAGATAACACAATGC3' and 5'CTGAGCCTTCTTCGGGTCCAGG3'). The 2042 bp product was visualized by agarose gel electrophoresis.

Growth conditions and inhibitor treatments

Inhibitor treatment experiments were performed according to Collings *et al.* (2006). Seed germination was synchronized by several days at 4 °C, followed by growth on vertical Murashige and Skoog (MS) plates for 4–5 d at 22 °C with a 16 h light/8 h dark cycle prior to transfer on inhibitor-containing media, which were then incubated under the same conditions for 72 h, unless stated otherwise. Inhibitor stock solutions were prepared in dimethylsulphoxide (DMSO), stored at −20 °C [latrunculin B (LatB), oryzalin (Oryz), taxol, and jasplakinolide] or 4 °C (SMIFH2), and added to liquid agar to the desired concentrations; the DMSO concentration was adjusted to 0.2% (v/v). All inhibitors were purchased from Sigma. Effective doses were calculated using the R statistical software (http://www.r-project.org/index.html) according to Knezevic *et al.* (2007) from two or three replications of ~20 plants for each concentration.

Morphometric analyses

Root diameter and root growth (defined as increment in length in a specified interval of time) was determined from photographs taken at 24, 48, and 72 h after transfer with a digital camera (Olympus C5050), measuring the distances between the root tips and marks made on the rear of the plates at tip locations at transfer time. To determine root hair density, root hairs were counted under a light microscope (BX-51, Olympus) at ×10 magnification in a 2 mm region at the midpoint of the portion of root grown after transfer. Lengths of 10 root hairs from the midpoint of each measured region were measured at ×20 magnification. From the same zone, root diameter and the lengths of 10 trichoblasts and 10 atrichoblasts per root were estimated. In all experiments, 2–3 replicates of ~20 plants were used per data point. Measurements were performed using the ImageJ software (http://rsbweb.nih.gov; Abramoff *et al.,* 2004).

Confocal microscopy and image analysis

GFP-tagged cytoskeleton was observed in roots of 5-day-old seedlings using a confocal laser scanning microscope (LCS 510; Leica) with a ×63/1.2 water immersion objective and 488 nm argon laser (25 mW) excitation. Images were acquired as z-series with a 0.7–1 µm interval. Microfilament bundling and density were quantified according to van der Honing *et al*. (2012) and Higaki *et al.* (2010). Profiles of fluorescence intensity were divided into four classes of grey level (arbitrary units) to generate plots documenting microfilament bundling (low intensity represents weakly labelled bundles or single filaments; high intensity corresponds to brightly labelled bundles). Skewness of fluorescence intensity distribution (correlated with microfilament bundling because bundles exhibit brighter fluorescence) and occupancy (i.e. fraction of pixels constituting the skeletonized microfilaments relative to the total pixel number of the analysed region, proportional to the overall microfilament density) were determined using the ImageJ plugins and macros from Higaki´s laboratory (http:/hasezawa.ib.k.u-tokyo.ac.jp/zp/Kbi/HigStomata). Microtubule density was determined as the number of microtubules in an area of 500 µm^2 from confocal images in five cells from several plants.

VAEM

To evaluate cytoskeletal dynamics, we used the Leica AF6000 LX fluorescence platform with integrated TIRF module, the HCX PL APO ×100/1.46 oil immersion objective, 400 nm peak excitation, and 210 ms exposure time. Plants were mounted in water on chambered slides; images were captured with a Leica DFC350FXR2 digital camera at 0.5 s intervals over the course of 2 min and analysed with Leica Application

Suite (LAS) and ImageJ software. Kymographs were generated using the Multiple Kymograph ImageJ plug-in from a time-lapse image series collected from well-focused 30 µm long 'optical transects' parallel to the longitudinal axis of the root (Sampathkumar *et al.,* 2011). The distribution of microtubule growth and shrinkage rates was estimated from at least 250 microtubule ends from at least 50 atrichoblasts in each genotype or treatment.

Results

Cytoskeletal inhibitors differentially affect root growth in fh1 *mutant and wild-type seedlings*

Two *Arabidopsis* T-DNA mutant lines, *fh1-1* and *fh1-2*, with corresponding wt controls were characterized. The T-DNA insertion interrupts the *AtFH1* gene in the third exon in *fh1-1* and in the 5' untranslated region (UTR; 27 bp before start codon) in *fh1-2* (Fig. 1A). In homozygous seedlings, AtFH1 mRNA was undetectable in *fh1-1*, while *fh1-2* had a reduced transcript level (Fig. 1B).

Under standard growth conditions in soil or *in vitro*, *fh1-1* and *fh1-2* plants do not differ noticeably from the wt. The *in vitro* growth media were thus supplemented with anti-cytoskeletal drugs LatB and/or Oryz to enhance expected subtle cytoskeletal defects and uncover novel mutant phenotypes.

At 0.1 µM concentration, the actin polymerization inhibitor LatB caused a more severe increase in root diameter and reduction in the longitudinal root growth rate in young seedlings of both mutant lines compared with the wt; the difference developed gradually within the first 48 h on LatB (Fig. 2). Higher concentrations severely affected both genotypes, and the difference between the mutant and wt was no longer significant (Supplementary Fig. S1A, B available at *JXB* online).

While the microtubule-depolymerizing drug Oryz also caused root thickening and reduced root growth, its effect was similar in both *fh1* and wt seedlings. (Supplementary Fig. S1C, D at *JXB* online). However, simultaneous addition of 0.33 µM LatB (i.e. a concentration that equally affected mutant and wt roots) increased the sensitivity of *fh1* mutants to a low concentration of Oryz compared with the wt (Supplementary Fig. S1E).

Next, the inhibitor concentrations at which root diameter showed half the maximal increase (D_{50}) and at which roots showed a 50% reduction in growth rate (L_{50}) were estimated from dose–response curves of mutant and wt seedlings. Radial root expansion was always more sensitive to inhibitors than longitudinal growth. For LatB, both D_{50} and L_{50} were significantly lower in the *fh1* mutants than in the wt (Table 1).

Treatment with cytoskeleton-stabilizing drugs (jasplakinolide for actin or taxol for microtubules) resulted in reduced root growth and increased diameter in both *fh1-1* mutant and wt seedlings. Both genotypes responded similarly, although longitudinal growth of mutant roots was significantly less affected by taxol (Supplementary Fig. S2 at *JXB* online).

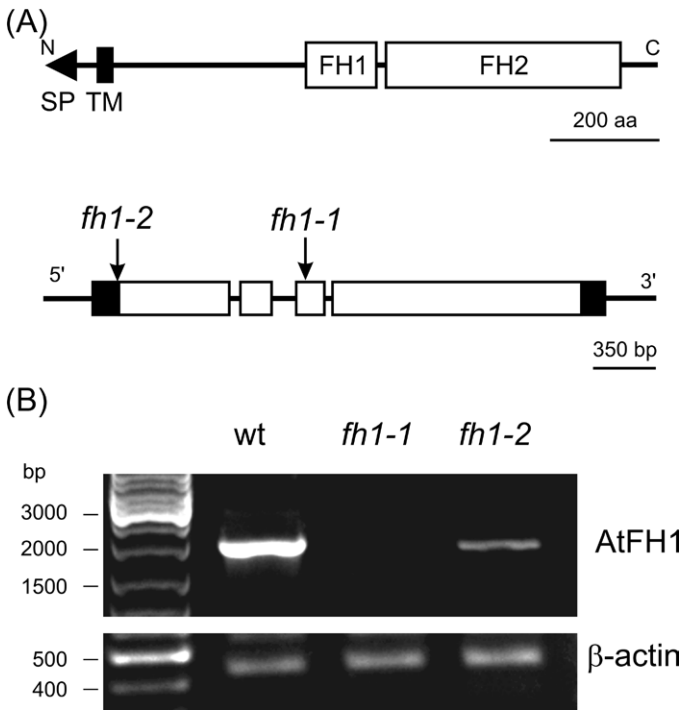

Fig. 1. The *AtFH1* (At5g25500) locus and mutants. (A) AtFH1 protein domain structure (above); map of the *AtFH1* gene and location of T-DNA insertions (below: open boxes, coding exons; filled boxes, non-coding exons; lines, introns and non-transcribed sequences). (B) *AtFH1* transcripts in wt and homozygous mutant seedlings determined by semi-quantitative RT–PCR.

Cytoskeletal inhibitors affect cell expansion and root hair development in mutants

Reduced longitudinal root growth can be due to impaired cell division or elongation, or both. To evaluate the contribution of cell elongation, the length of mature trichoblasts and atrichoblasts in inhibitor-treated roots was measured. LatB-grown *fh1-1* and *fh1-2* roots had shorter, wider cells, suggesting that the phenotype is at least partly due to more isodiametric cell growth (Fig. 3A, B; Supplementary Table S1 at *JXB* online).

Mutant rhizodermis cells, especially trichoblasts, were often mis-shapen, exhibiting bulbous structures at root hair bases and/or branched root hairs (Fig. 3C). A significantly higher density of both total and abnormal root hairs was found in mutant, but not wt, seedlings grown on 0.1 µM LatB compared with drug-free control, apparently due to shorter trichoblasts. At 0.33 µM LatB, the total number of root hairs was reduced in both genotypes; mutants had more abnormal root hairs than the wt. A further increase in the LatB concentration completely inhibited root hair development. While *fh1* mutants showed, on average, longer root hairs than the wt on control media or 0.1 µM LatB or Oryz, their root hairs were shorter on 0.33 µM LatB, suggesting increased sensitivity of tip growth to higher LatB doses. However, since root hair length varied substantially, the biological significance of this observation is questionable (Fig. 3D; Supplementary Table S1 at *JXB* online).

Actin and microtubule distribution in fh1 *mutants*

In the above experiments, both *fh1* alleles behaved similarly, though *fh1-1* had more pronounced phenotypes, in

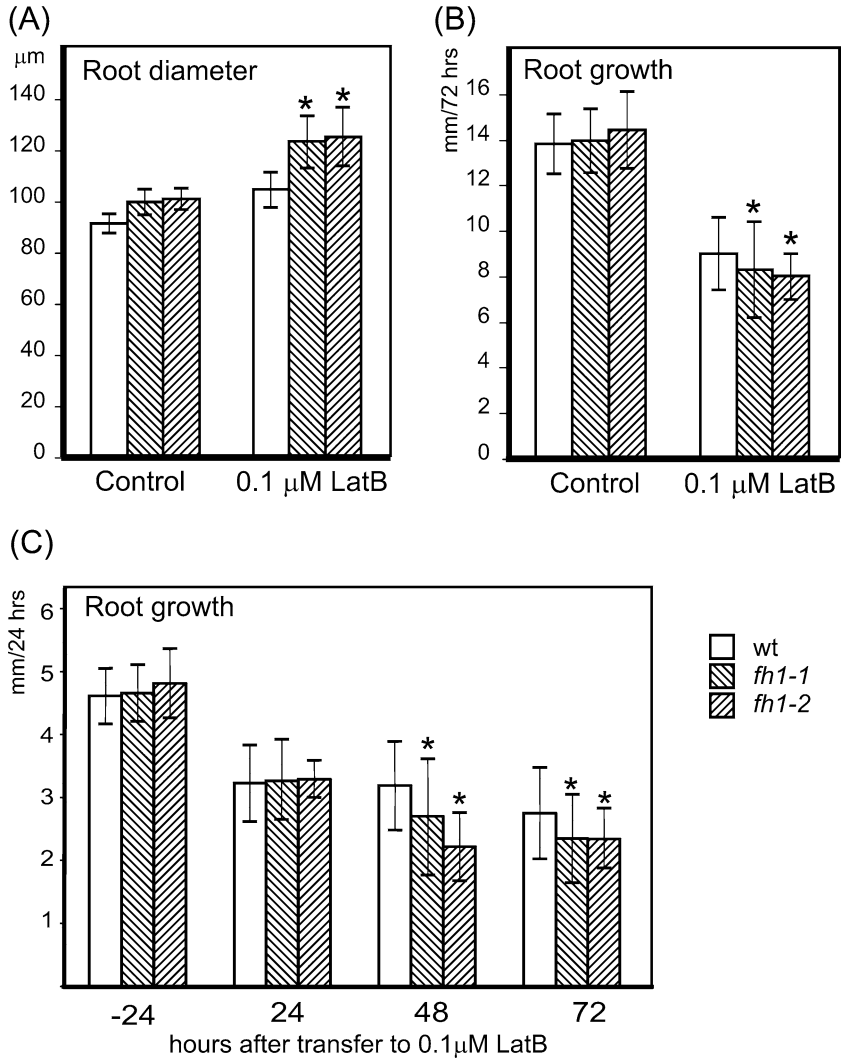

Fig. 2. Mutants lacking *AtFH1* exhibit thicker, slower growing roots than the wt when treated with 0.1 µM LatB. (A) Root diameter and (B) incremental root growth during 72 h after transfer to LatB. Significant differences between any of the mutants and the wt in root diameter (*t*-test $P < 0.0001$) or root growth (*t*-test $P < 0.05$) are marked by asterisks. (C) Gradual decrease in root growth rates after 24, 48, and 72 h on LatB. Significant differences between mutant and wt seedlings (*t*-test $P < 0.0001$) are marked by asterisks; data from the last 24 h before transfer are shown for control.

agreement with the residual gene expression in *fh1-2*. *fh1-1* was thus chosen for introduction of *in vivo* fluorescent protein-tagged cytoskeletal markers (GFP–FABD for actin and GFP–MAP4 for microtubules) by crossing. Sister segregants carrying wt AtFH1 were used as controls.

Table 1. Effective doses of LatB and Oryz in mutants and the wild type.

Treatment	D_{50}		L_{50}	
	fh1-1	Wt	*fh1-1*	Wt
Lat B	10.1**	28.3	131.6**	163.7
Oryz	96*	114.4	233.1	224.3

D_{50}, inhibitor concentration causing response half way between zero and the maximal observed diameter increase; L_{50}, inhibitor concentration causing response half way between zero and the maximal observed growth reduction.
*Significant difference from the wt at $P < 0.05$; **significant difference from the wt at $P < 0.001$.

The effects of the markers themselves on root growth in both *fh1-1* and the wt were examined. GFP–MAP4 caused root thickening and reduction of root growth, and induced left-handed root twisting, as described previously (Granger and Cyr, 2001; Hashimoto, 2002); these effects were less pronounced in *fh1-1*mutants than in the wt. GFP–FABD did not show any significant effects in either *fh1-1* or wt seedlings (Supplementary Fig. S3 at *JXB* online).

Given that this study was looking at root development, the focus here was on *in vivo* observations in rhizodermal cells. Thicker and more frequent actin bundles were usually observed in *fh1* mutants than in wt seedlings. Low doses of LatB did not disrupt filaments but rather increased actin bundling, more obviously in mutants than in wt plants. LatB-treated wt plants thus somewhat resembled *fh1* mutants grown under control

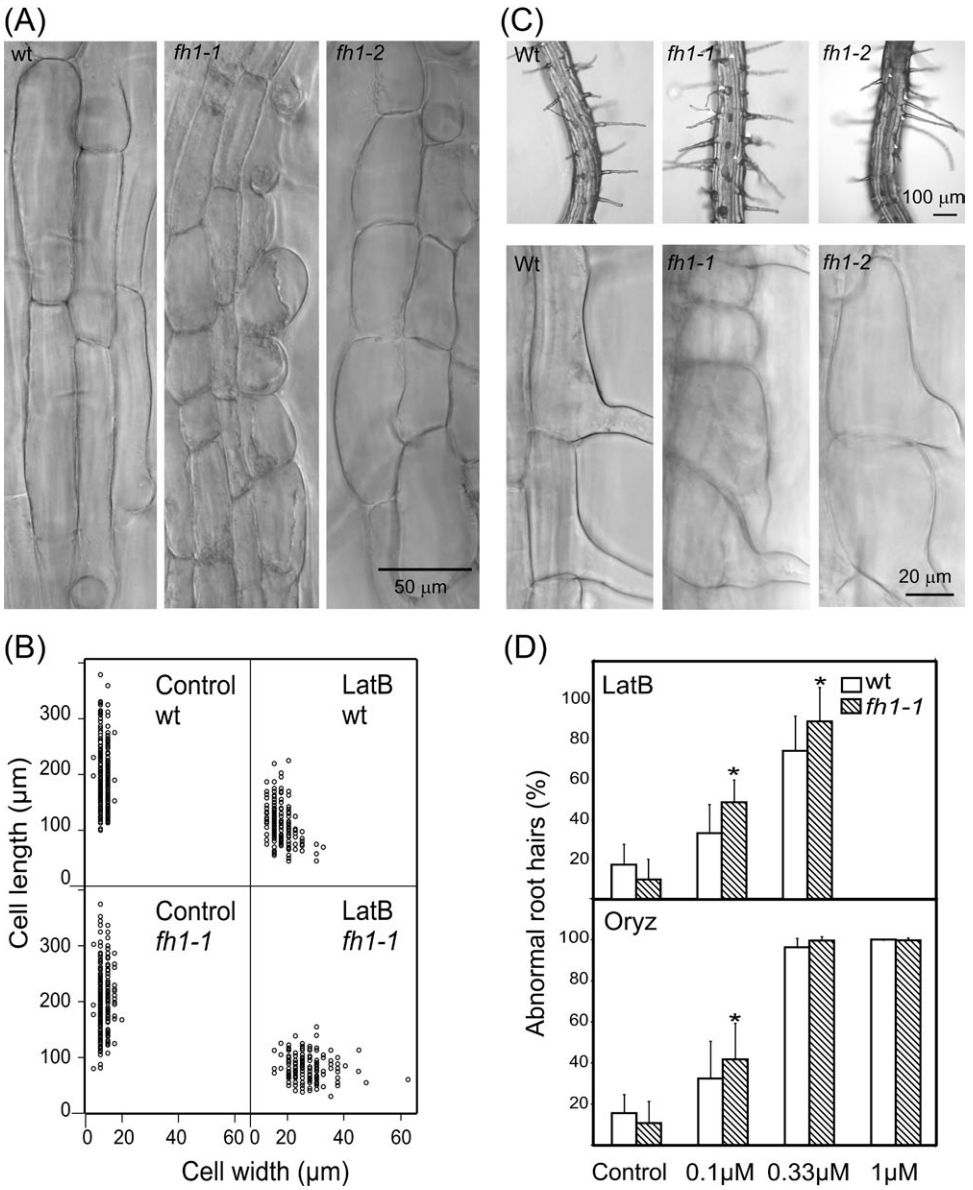

Fig. 3. Effects of LatB on rhizodermis and root hair development in *fh1* mutant and wt seedlings. (A) Typical appearance of elongation zone rhizodermis in wt and mutants exposed to LatB. (B) Relationship between mature rhizodermis cell length and width in *fh1-1* mutant and wt seedlings in control conditions and on 0.1 μM LatB (each sample contains equal numbers of trichoblasts and atrichoblasts); compare Supplementary Table S1 at *JXB* online for *fh1-2*. (C) Abnormal root hairs found in mutant but not wt plants grown on 0.1 μM LatB. (D) Percentage of abnormal root hairs in *fh1-1* and wt plants grown in LatB- and Oryz-supplemented media. Significant differences (*t*-test $P < 0.001$) are marked by an asterisk.

conditions (Fig. 4A). Quantification of the microfilament patterns in the rhizodermis of seedlings growing on control media by estimating the skewness of fluorescence intensity distribution (correlated with the level of microfilament bundling) and pixel occupancy (giving insight into the overall density of actin cytoskeleton) showed that mutants have fewer but thicker microfilaments, consistent with increased actin bundling (Fig. 4B). The differences are even more obvious in profiles of individual bundle fluorescence intensity (Fig. 4C), confirming that *fh1* mutants have fewer weakly labelled thin bundles or single filaments, and more bright thick bundles than wt plants.

Surprisingly, differences in microtubule organization between the wt and mutants were more pronounced than those in microfilaments. Even on control media, and more obviously in LatB-treated plants, mutants had fewer microtubules, shorter and less organized compared with the wt (Fig. 4D). Quantitative measurements of microtubule density revealed a significant reduction in LatB-treated *fh1* mutants compared with the wt (Fig. 4E).

Effect of fh1 *mutation on cytoskeletal dynamics monitored by VAEM*

To compare individual microfilament and microtubule dynamics in rhizodermis cells of wt and *fh1* mutant plants carrying GFP–FABD and GFP–MAP4, the VAEM technique was

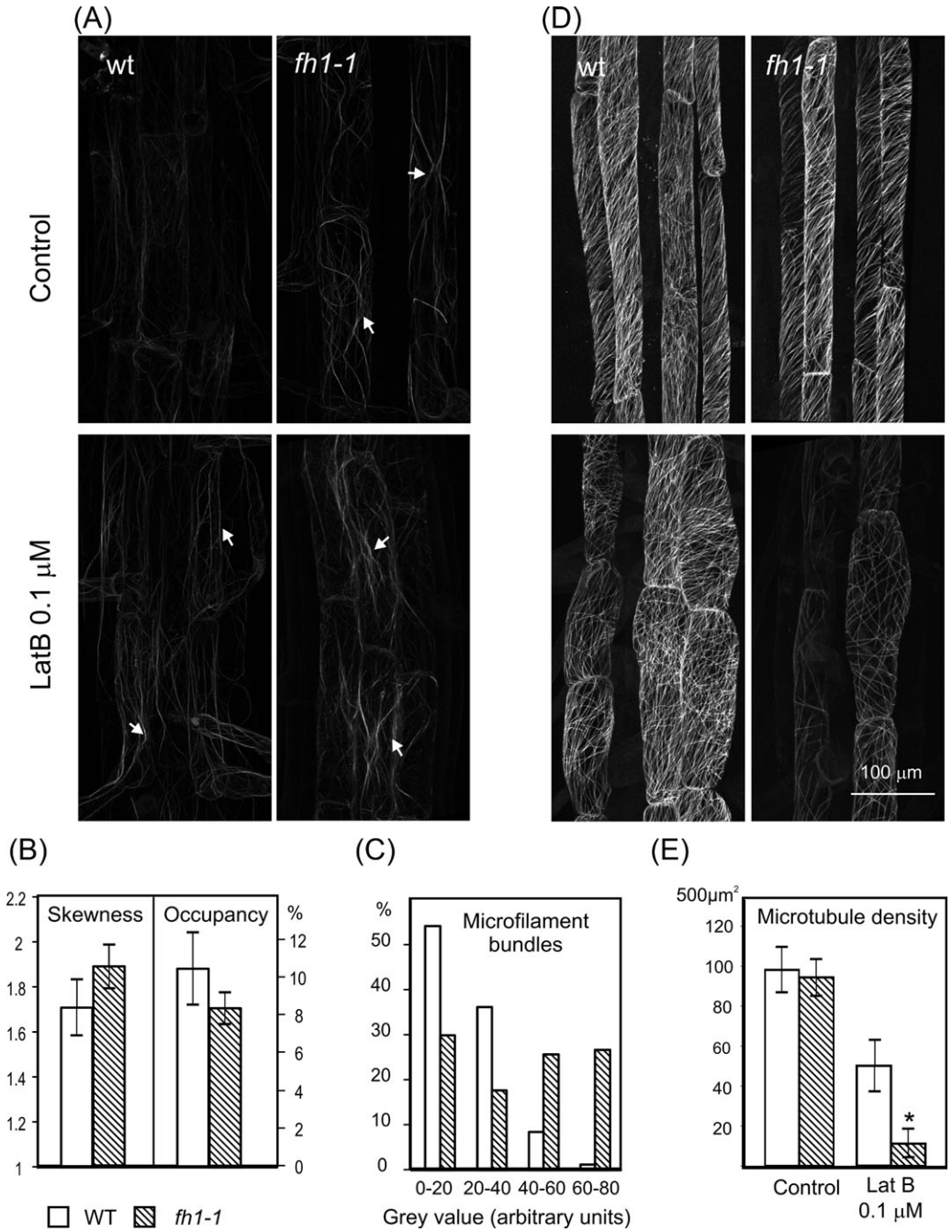

Fig. 4. Typical cytoskeleton organization in the rhizodermis of *fh1-1* mutant and wt seedlings. (A) Actin labelled by GFP–FABD; arrows, actin filament bundles. (B) Actin filament bundling (skewness) and density (occupancy) under control conditions. (C) Frequency distribution of actin fluorescence peaks in four fluorescence intensity classes under control conditions. (D) Microtubules labelled by GFP–MAP4. (E) Microtubule density. Significant differences (*t*-test $P < 0.001$) are marked by an asterisk.

employed. Since preliminary experiments indicated that the three developmental zones of the root tip differ in cytoskeletal dynamics, the beginning of the differentiation zone was investigated, where both cytoskeletal systems behaved consistently very dynamically.

Differences in actin dynamics were observed between *fh1* mutants and the wt (Fig. 5; Supplementary Video S1, S2 at *JXB* online). Mutant microfilament bundles were more abundant and less dynamic (in particular, they remained longer at pause) than those of wt seedlings, except a few rapidly moving bundles. This might reflect differences either in bundle size or in the degree of actin cross-linking.

Differences between mutant and wt plants were also observed in microtubule dynamics (Fig. 6; Supplementary Video S3, S4 at *JXB* online). On the control medium, mutant microtubules exhibited increased dynamic instability compared with wt seedlings. LatB increased microtubule dynamics in both genotypes (Fig. 6A, B).

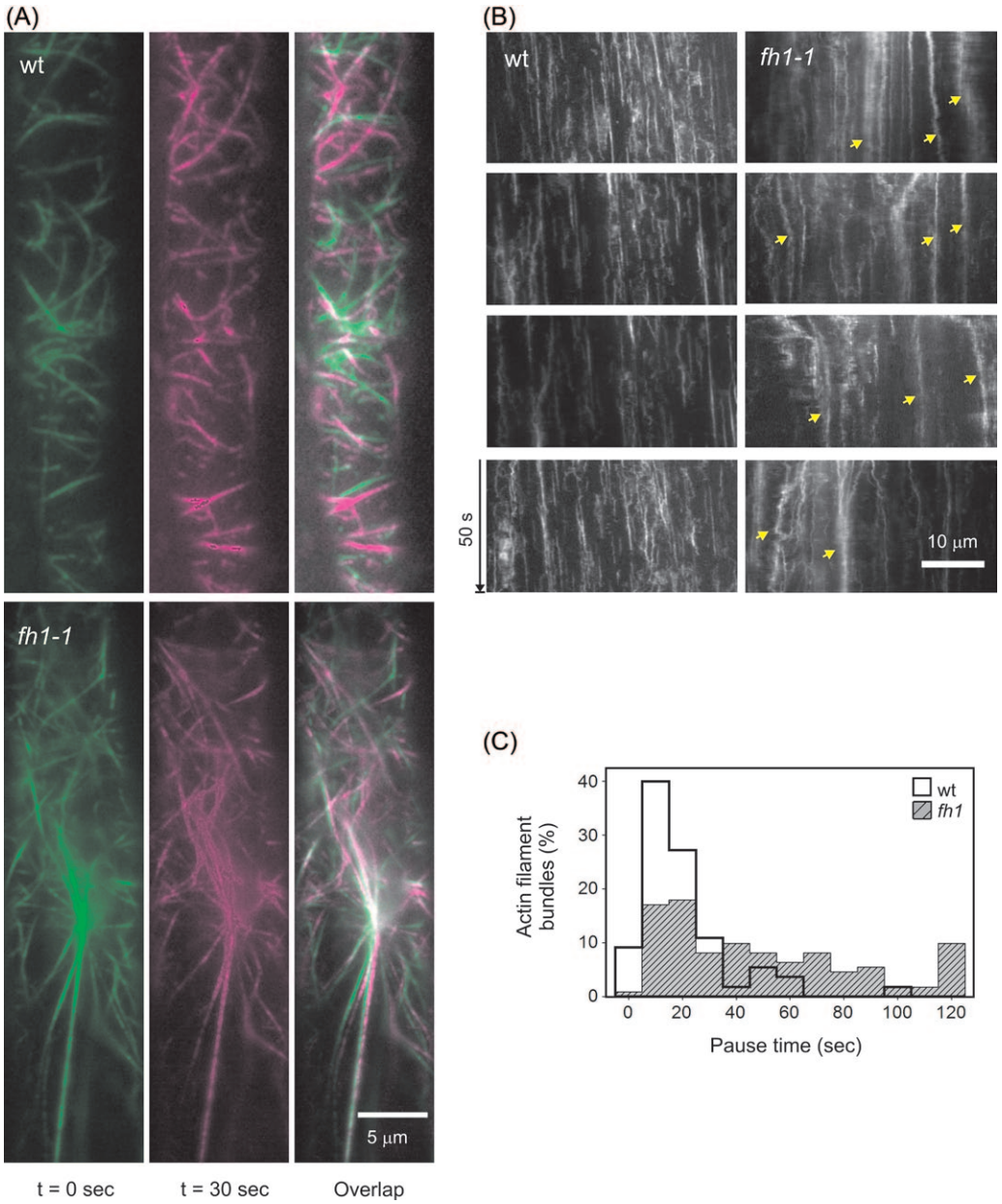

Fig. 5. GFP–FABD-tagged microfilament distribution and dynamics in the rhizodermis of *fh1-1* and wt seedlings on standard medium. (A) VAEM images from two time points and their overlap showing growing or moving filaments in magenta, shrinking in green, and pausing and growing/shrinking in light green and light magenta, respectively. (B) Kymograph showing the static thick actin bundles in the mutant (arrows). (C) Distribution of actin bundle pause duration in mutant and wt.

To quantify microtubule turnover, the distribution of microtubule phases was determined in images taken during the time span of 2 min. Mutants had fewer shrinking or pausing microtubules but more microtubules undergoing stochastic transition (i.e. alternatively shrinking and growing) than the wt (Fig. 6C). LatB reduced the fraction of growing microtubules in both genotypes, and increased the fraction of growing/shrinking microtubules even in the wt (again, LatB-treated wt plants resembled *fh1* mutants grown under control conditions). Oryz in both genotypes increased the percentage of pausing microtubules and reduced the growing, shrinking, and growing/shirinking fractions. The distribution of microtubule growth and shrinkage rates differed somewhat between *fh1* and wt roots (Supplementary Fig. S4 at *JXB* online). Despite comparable average growth rates, a higher proportion of microtubules in *fh1* cells grew more slowly than average; this difference persisted upon LatB treatment, while Oryz reduced the growth rate in both the *fh1* mutant and the wt.

Effects of the formin inhibitor SMIFH2 mimic the fh1 *mutation*

To verify that the observed mutant phenotypes are due to disrupted formin function, the effects of a recently described inhibitor of formin-mediated actin assembly, SMIFH2 (Rizvi

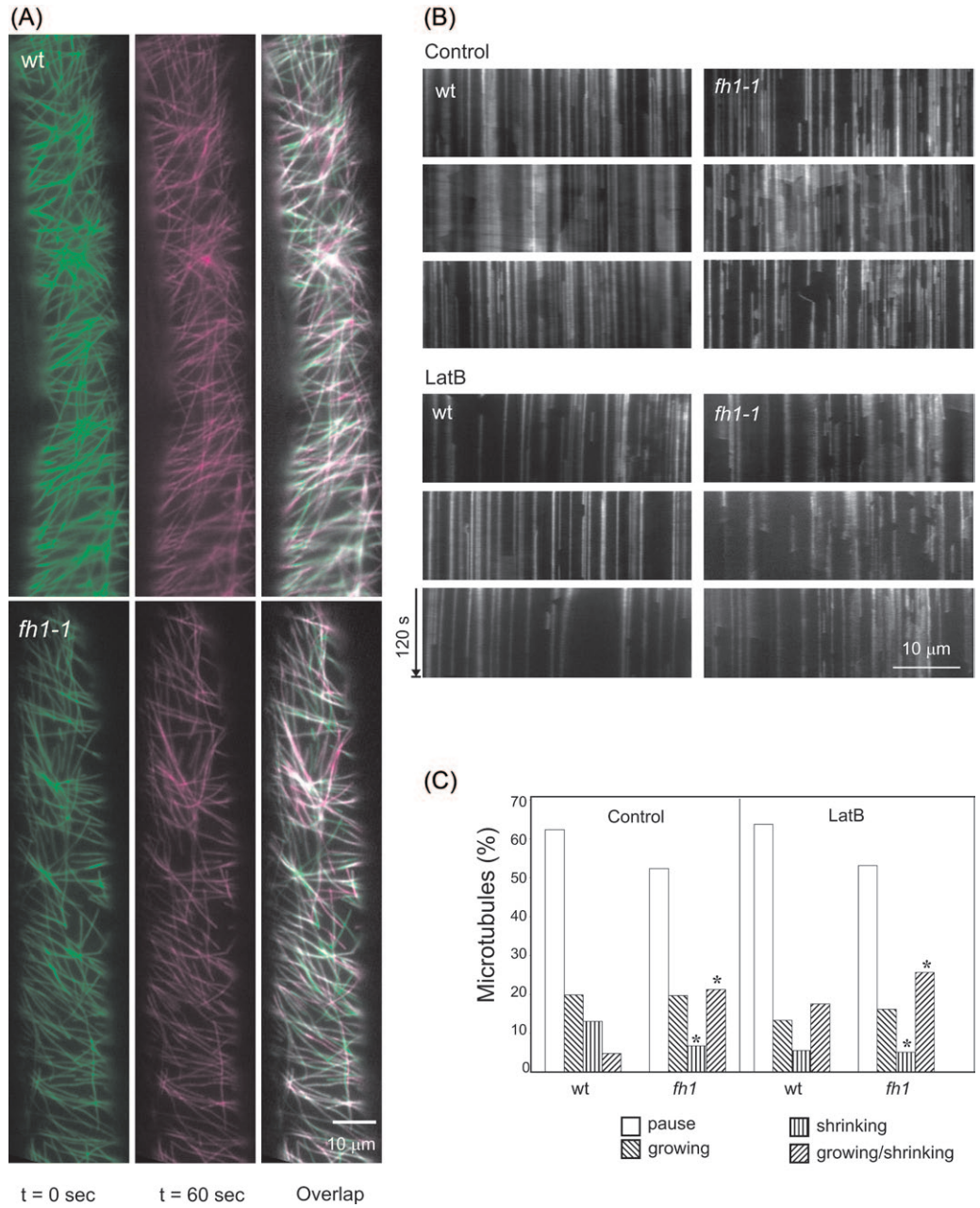

Fig. 6. GFP–MAP4-tagged microtubule distribution and dynamics in *fh1-1* mutant and wt rhizodermis. (A) VAEM images from two time points and their overlap showing growing microtubules in magenta, shrinking in green, pausing in light green, and growing/shrinking in light magenta. (B) Kymographs of microtubule dynamics under control conditions and on 0.1 µM LatB-supplemented medium. (C) Distribution of microtubule phases on control and 0.1 µM LatB-containing media. An asterisk indicates a significant difference between mutants and the wt (*t*-test $P < 0.0001$).

et al., 2009), were examined in wt seedlings. In the standard experimental set-up, significant reduction of root growth was observed at or above a concentration of 20 µM in both the wt and *fh1* mutants (Fig. 7A). The effect of SMIFH2 was stronger when seedlings were exposed to the drug in the dark (possibly due to light sensitivity of the drug), and *fh1-1* mutant roots were significantly more affected than those of the wt (Supplementary Fig. S5 at *JXB* online). SMIFH2-treated wt seedlings expressing GFP–FABD and GFP–MAP4 exhibited increased microfilament bundling and reduced microtubule density, especially after additional LatB treatment, again reminiscent of *fh1* mutants (Fig. 7B).

Discussion

The first description is presented of a mutant phenotype in *A. thaliana* lacking the most expressed housekeeping class I formin, AtFH1. It is shown that AtFH1 affects actin and microtubule dynamics, processes central for cell expansion and development.

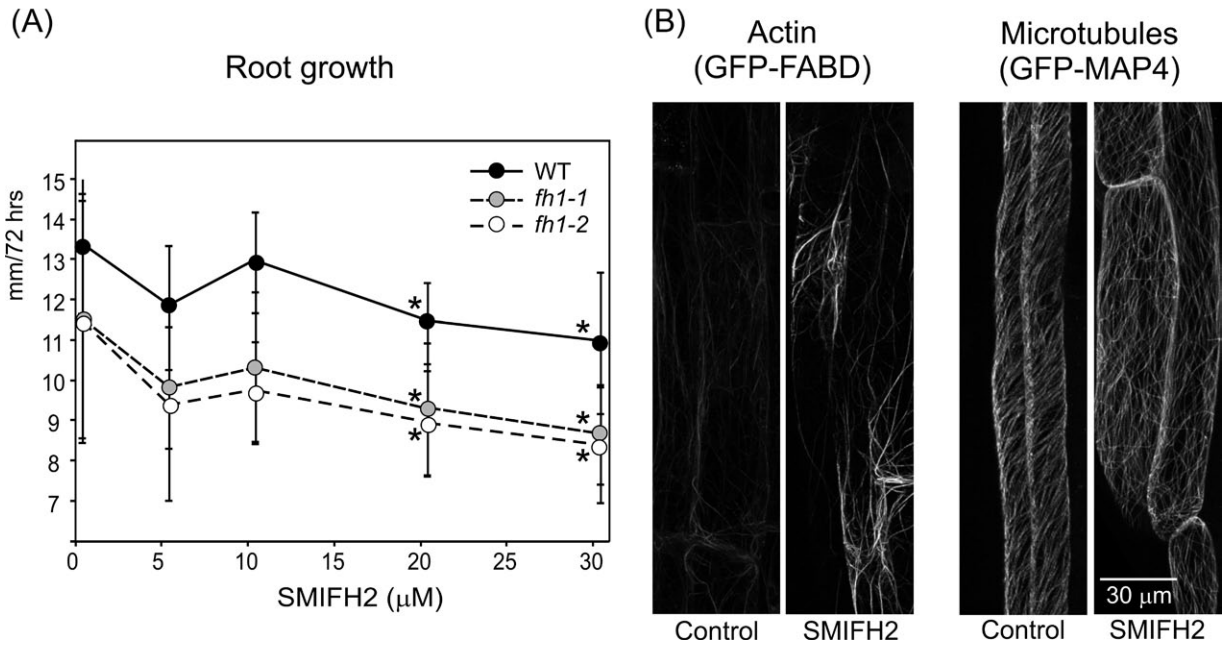

Fig. 7. Effects of SMIFH2 on longitudinal root growth and cytoskeletal organization. (A) Concentration-dependent growth inhibition; asterisks denote significant differences from non-treated seedlings of the same genotype (*t*-test $P < 0.0001$). (B) Rhizodermal microfilament and microtubule organization under control conditions and on 20 μM SMIFH2-supplemented medium.

Using cytoskeletal inhibitors to uncover mutant phenotypes

Angiosperm FH2 proteins form a large family of paralogues: *A. thaliana* has 21 formin-encoding genes, 11 of them in class I. Ten of these (including AtFH1) share the characteristic clade-specific domain structure (Deeks *et al.,* 2002; Grunt *et al.,* 2008). Loss of a single formin gene thus rarely causes obvious phenotypic effects due to 'functional redundancy'. Only subtle, if any, phenotypes have so far been documented for loss-of-function class I formin mutants. Such phenotypes are usually tissue specific, reflecting the pattern of gene expression. Loss of AtFH5 caused delayed endosperm cytokinesis (Ingouff *et al.,* 2005), and pollen tube defects were elicited by RNA interference (RNAi) targeting the pollen formins AtFH3 in *Arabidopsis* or NtFH5 in tobacco (Ye *et al.,* 2009; Cheung *et al.,* 2010). Additional phenotypes were produced by overexpression, sometimes ectopic or heterologous, of wt or mutant proteins, such as AtFH1 (Cheung and Wu, 2004) or AtFH8 (Deeks *et al.,* 2005; Yi *et al.,* 2005).

Asymptomatic or mildly symptomatic doses of inhibitors of specific cellular functions may result in a 'synthetic phenotype' in mutants where the inhibitor's target(s) are already weakened. In mutants of *Arabidopsis* formins AtFH8 (Xue *et al.,* 2011) and AtFH12 (Cvrčková *et al.,* 2012), LatB induced alterations in roots and/or root hairs. In the present report, the response of T-DNA mutants with insertions in AtFH1 to cytoskeletal inhibitors targeting either actin (LatB) or microtubules (Oryz) was examined, since no readily noticeable differences between *fh1* mutants and the wt were observed under control conditions.

Low doses of LatB, inhibiting primary root growth and causing radial swelling in young seedlings, and enhancing the phenotype of some cytoskeletal mutations (Collings *et al.,* 2006), affected the *fh1* mutants more than the wt. However, the whole organ phenotype was subtle compared with effects on the level of individual cells or cytoskeletal structures, providing yet another example of organ- and tissue-level compensation of cell-level defects (see Breuninger and Lenhard, 2010). The shorter, thicker roots of LatB-treated mutants consisted of shorter and wider cells, suggesting altered cell expansion rather than cell division, consistent with previous observations (Baluška *et al.,* 2001). LatB can also disrupt intracellular membrane trafficking (Zhang *et al.,* 2010), crucial for polar auxin transport. Since auxin, in turn, affects actin, it is difficult to separate direct and auxin-mediated effects on root growth (Rahman *et al.,* 2007).

LatB-treated *fh1* mutants also exhibited malformed root hairs. Unlike pollen tubes ectopically overexpressing AtFH1, which have bulbous tips (Cheung and Wu, 2004), in the experiments presented here, mainly root hair bases were affected, resembling the phenotype of actin (*act2*) mutants (Gilliland *et al.,* 2002; Nishimura *et al.,* 2003) and suggesting defective focusing of exocytosis during the bulge stage.

Disruption of microtubules affected *fh1* mutants and the wt similarly, consistent with AtFH1 functioning mainly through actin. However, mutants exhibit increased sensitivity to Oryz in the presence of LatB, suggesting that AtFH1 may participate in a cross-talk between microfilaments and microtubules, and that its loss might, under some circumstances, destabilize microtubules. Consistently, mutants are partially resistant towards the root growth inhibition, radial root swelling, and root twisting induced by the GFP–MAP4 marker and taxol, which can stabilize and bundle microtubules (Granger and Cyr, 2001; Hashimoto, 2002).

Formin inhibition mimics the mutant phenotype

The small molecule SMIFH2, a 2-thio-oxodihydropyrimidine-4,6-dione derivative, is an inhibitor of FH2 domain-mediated actin assembly, active *in vitro* against several formins, and eliciting actin-related phenotypes in yeast and mammalian cells (Rizvi *et al.,* 2009). Its *in vitro* characterized targets represent sufficiently distant formin clades (see Grunt *et al.,* 2008) to suggest that SMIFH2 should inhibit most or all formins.

In the present study, SMIFH2 reduced root growth, increased microfilament bundling, and decreased cortical microtubule density; that is, it mimicked some phenotypes observed in *fh1* mutants (especially after LatB treatment). Consistent with SMIFH2 also targeting the remaining formins, *fh1* mutants were still responding to the inhibitor. The stronger mutant allele, *atfh1-1*, was even somewhat more sensitive towards root growth inhibition in the dark, reminiscent of increased sensitivity of some cytoskeletal mutants to inhibitors (see above). While non-specific effects of SMIFH2 cannot be ruled out, as its reported inactive analogue (Rizvi *et al.,* 2009) is not commercially available, the present observations support the notion that the mutant phenotypes are indeed due to perturbation of formin function.

Changes in actin and microtubule distribution and dynamics in fh1 *mutants*

Plant actin and microtubule networks undergo constant remodelling (Staiger *et al.,* 2009; Blanchoin *et al.,* 2010). They are mutually interdependent, and sometimes co-aligned; microtubule-disrupting drugs may affect actin organization, and vice versa (Collings *et al.,* 2006; Smertenko *et al.,* 2010; Sampathkumar *et al.,* 2011). The actin–microtubule 'cross-talk' may be mediated by bifunctional proteins or protein complexes (see Petrášek and Schwarzerová, 2009).

The thicker, more compact actin bundles in the *fh1* mutants are reminiscent of some *Arabidopsis* mutants with an altered balance between fine actin filaments and bundles, such as *adf4* (Henty *et al.,* 2011) or *aip1* (Ketelaar *et al.,* 2004). AtFH1 might stabilize microfilaments by bundling (Michelot *et al.,* 2005, 2006), enhanced polymerization, or capping, as reported for its relative AtFH8 (Yi *et al.,* 2005). Low doses of LatB also disrupt fine actin filaments, resulting in increased actin bundling and reduced stochastic dynamics (Staiger *et al.,* 2009). It is thus not surprising that LatB enhanced the effects of the *fh1* mutation and mimicked its phenotype in wt plants. Consistent with AtFH1 participating in actin–microtubule cross-talk, LatB also aggravated or phenocopied the presumably microtubule-related cell expansion phenotypes.

To gain insight into cytoskeletal dynamics in wt and mutant plants, VAEM, a fluorescence microscopy technique allowing time-lapse imaging of a thin cortical layer of the cytoplasm, recently also adopted in plants (Smertenko *et al.,* 2010; Sparkes *et al.,* 2011; Vizcay-Barrena *et al.,* 2011; Wan *et al.,* 2011), was used. Increased bundling and decreased dynamics of the cortical actin in *fh1* mutants were observed, suggesting altered actin-bundling, capping, or severing activities. Indeed, some formins can sever actin (Harris *et al.,* 2004; Yi *et al.,* 2005), thereby contributing to overall actin mobility, and AtFH1 may also have this ability. AtFH1 also anchors actin filaments across the plasmalemma into the cell wall (Martiniere *et al.,* 2011), which may effectively constrain bundling.

As suggested already by the root growth phenotypes discussed above, *fh1* mutants exhibited increased microtubule dynamics (important for cell elongation; Shaw *et al.,* 2003), although the plus-end growth rates were remarkably decreased. There are multiple documented cases of formins participating in actin–microtubule cross-talk or binding to microtubules (Bartolini and Gundersen, 2010; Chesarone *et al.,* 2010).

Particular microtubule-binding motifs may be restricted to narrow formin lineages (Deeks *et al.,* 2010; Li *et al.,* 2010; Yang *et al.,* 2011; Zhang *et al.,* 2011). Formins might also bind microtubules indirectly via heterodimerization with tubulin-binding paralogues, though heterodimerization is so far documented only among closely related mammalian Diaphanous formins (Copeland *et al.,* 2007). The microtubule-related effects may also be mediated by other microtubule-associated proteins; co-expression of AtFH1 with the At3g16060 kinesin (see data from http://string-db.org; Szklarczyk *et al.,* 2011) is interesting in this respect. However, since AtFH1 is excluded from the areas of cell cortex occupied by microtubules (Martiniere *et al.,* 2011), the effects on microtubule dynamics may be secondary to those on microfilaments.

In summary, phenotypic effects of loss of function of AtFH1, which altered root cell expansion, root hair morphogenesis, and cytoskeletal dynamics especially under conditions perturbing the actin cytoskeleton, were documented. Consistent effects were also elicited by the formin inhibitor SMIFH2. These results suggest the participation of AtFH1 in actin–microtubule cross-talk *in vivo* by an as yet unclear mechanism.

Supplementary data

Supplementary data are available at *JXB* online.

Table S1. Trichoblast, atrichoblast, and root hair characteristics in inhibitor-treated wt and mutant seedlings.

Figure S1. Dose–response curves of wt and *fh1-1* root growth parameters for varying concentrations of cytoskeletal inhibitors.

Figure S2. Effects of taxol and jasplakinolide on wt and *fh1-1* root growth.

Figure S3. Effects of GFP–MAP4 and GFP–FABD on wt and *fh1-1* root growth.

Figure S4. Distribution of microtubule growth and shrinkage rates in *fh1-1* mutant and wt seedlings.

Figure S5. Effects of SMIFH2 on wt and *fh1* root growth under dark conditions.

Video S1. Actin dynamics in wt rhizodermis under control conditions.

Video S2. Actin dynamics in *fh-1* rhizodermis under control conditions.

Video S3. Microtubule dynamics in wt rhizodermis under control conditions.

Video S4. Microtubule dynamics in *fh1-1* rhizodermis under control conditions.

Acknowledgements

This work was supported by the MSM 0021620858, GACR P305/10/0433, and SVV 265203 projects. We thank Aleš Soukup, Ondřej Šebesta, and Ondřej Horvath for help with microscopy and image analysis, Marta Čadyová for technical support, and two anonymous reviewers for helpful comments.

References

Abe T, Hashimoto T. 2005. Altered microtubule dynamics by expresion of modified alfa-tubulin protein causes right-handed helical growth in transgenic Arabidopsis plants. *The Plant Journal* **43,** 191–204.

Abramoff MD, Magelhaes PJ, Ram SJ. 2004. Image processing with ImageJ. *Biophotonics International* **11,** 36–42.

Alonso J, Stepanova A, Leisse T, *et al.* 2003. Genome-wide insertional mutagenesis of Arabidopsis thaliana. *Science* **301,** 653–657.

Baluška F, Jasik J, Edelmann H, Salajova T, Volkmann D. 2001. Latrunculin B-induced plant dwarfism: plant cell elongation is F-actin-dependent. *Developmental Biology* **231,** 113–124.

Bannigan A, Baskin T. 2005. Directional cell expansion—turning toward actin. *Current Opinion in Plant Biology* **8,** 619–624.

Banno H, Chua N. 2000. Characterization of the Arabidopsis formin-like protein AFH1 and its interacting protein. *Plant and Cell Physiology* **41,** 617–626.

Bartolini F, Gundersen G. 2010. Formins and microtubules. *Biochimica et Biophysica Acta* **1803,** 164–173.

Blanchoin L, Boujemaa-Paterski R, Henty J, Khurana P, Staiger C. 2010. Actin dynamics in plant cells: a team effort from multiple proteins orchestrates this very fast-paced game. *Current Opinion in Plant Biology* **13,** 714–723.

Blanchoin L, Staiger C. 2010. Plant formins: diverse isoforms and unique molecular mechanism. *Biochimica et Biophysica Acta* **1803,** 201–206.

Breuninger H, Lenhard M. 2010. Control of tissue and organ growth in plants. *Current Topics in Developmental Biology* **91,** 185–220.

Chesarone M, DuPage A, Goode B. 2010. Unleashing formins to remodel the actin and microtubule cytoskeletons. *Nature Reviews. Molecular Cell Biology* **11,** 62–74.

Cheung A, Niroomand S, Zou Y, Wu H. 2010. A transmembrane formin nucleates subapical actin assembly and controls tip-focused growth in pollen tubes. *Proceedings of the National Academy of Sciences, USA* **107,** 16390–16395.

Cheung A, Wu H. 2004. Overexpression of an Arabidopsis formin stimulates supernumerary actin cable formation from pollen tube cell membrane. *The Plant Cell* **16,** 257–269.

Cole R, Synek L, Žárský V, Fowler J. 2005. SEC8, a subunit of the putative Arabidopsis exocyst complex, facilitates pollen germination and competitive pollen tube growth. *Plant Physiology* **138,** 2005–2018.

Collings D, Lill A, Himmelspach R, Wasteneys G. 2006. Hypersensitivity to cytoskeletal antagonists demonstrates microtubule–microfilament cross-talk in the control of root elongation in Arabidopsis thaliana. *New Phytologist* **170,** 275–290.

Copeland S, Green B, Burchat S, Papalia G, Banner D, Copeland J. 2007. The diaphanous inhibitory domain/diaphanous autoregulatory domain interaction is able to mediate heterodimerization between mDia1 and mDia2. *Journal of Biological Chemistry* **282,** 30120–30130.

Cvrčková F. 2000. Are plant formins integral membrane proteins? *Genome Biology* **1**, RESEARCH001.

Cvrčková F, Grunt M, Žárský V. 2012. Expression of GFP–mTalin reveals an actin-related role for the arabidopsis class II formin AtFH12. *Biologia Plantarum* **3,** 431–440.

Deeks M, Cvrčková F, Machesky L, Mikitová V, Žárský V, Davies B, Hussey P. 2005. Arabidopsis group Ie formins localize to specific cell membrane domains, interact with actin-binding proteins and cause defects in cell expansion upon aberrant expression. *New Phytologist* **168,** 529–540.

Deeks M, Fendrych M, Smertenko A, Bell K, Oparka K, Cvrčková F, Žárský V, Hussey P. 2010. The plant formin AtFH4 interacts with both actin and microtubules, and contains a newly identified microtubule-binding domain. *Journal of Cell Science* **123,** 1209–1215.

Deeks M, Hussey P, Davies B. 2002. Formins: intermediates in signal-transduction cascades that affect cytoskeletal reorganization. *Trends in Plant Science* **7,** 492–498.

Dvořáková L, Cvrčková F, Fischer L. 2007. Analysis of the hybrid proline-rich protein families from seven plant species suggests rapid diversification of their sequences and expression patterns. *BMC Genomics* **8,** 412.

Emons A, Hofte H, Mulder B. 2007. Microtubules and cellulose microfibrils: how intimate is their relationship? *Trends in Plant Science* **12,** 279–281.

Gilliland L, Kandasamy M, Pawloski L, Meagher R. 2002. Both vegetative and reproductive actin isovariants complement the stunted root hair phenotype of the Arabidopsis act2-1 mutation. *Plant Physiology* **130,** 2199–2209.

Gilliland L, Pawloski L, Kandasamy M, Meagher R. 2003. Arabidopsis actin gene ACT7 plays an essential role in germination and root growth. *The Plant Journal* **33,** 319–328.

Granger CL, Cyr RJ. 2001. Spatiotemporal relationships between growth and microtubule orientation as revealed in living root cells of Arabidopsis thaliana transformed with green-fluorescent-protein gene construct GFP–MBD. *Protoplasma* **216,** 201–214.

Grunt M, Žárský V, Cvrčková F. 2008. Roots of angiosperm formins: the evolutionary history of plant FH2 domain-containing protein. *BMC Evolutionary Biology* **8,** 115.

Harris E, Li F, Higgs H. 2004. The mouse formin, FRL, slows actin filament barbed end elongation, competes with capping protein,

accelerates polymerization from monomers, and severs filaments. *Journal of Biological Chemistry* **279,** 20076–20087.

Hashimoto T. 2002. Molecular genetic analysis of left-right handedness in plants. *Philosophical Transactions of the Royal Society B: Biological Sciences* **357,** 799–808.

Henty J, Bledsoe S, Khurana P, Meagher R, Day B, Blanchoin L, Staiger C. 2011. Arabidopsis actin depolymerizing factor 4 modulates the stochastic dynamic behavior of actin filaments in the cortical array of epidermal cells. *The Plant Cell* **23,** 3711–3726.

Higaki T, Kutsuna N, Sano T, Kondo N, Hasezawa S. 2010. Quantification and cluster analysis of actin cytoskeletal structures in plant cells: role of actin bundling in stomatal movement during diurnal cycles in Arabidopsis guard cells. *The Plant Journal* **61,** 156–165.

Ingouff M, Fitz J, Guerin C, Robert H, Sorensen M, Van Damme D, Geelen D, Blanchoin L, Berger F. 2005. Plant formin AtFH5 is an evolutionarily conserved actin nucleator involved in cytokinesis. *Nature Cell Biology* **7,** 374–380.

Ketelaar T, Allwood E, Anthony R, Voigt B, Menzel D, Hussey P. 2004. The actin-interacting protein AIP is essential for actin organization and plant development. *Current Biology* **14,** 145–149.

Knezevic S, Streibig J, Ritz C. 2007. Utilizing R software package for dose–response studies: the concept and data analysis. *Weed Technology* **21,** 840–848.

Li Y, Shen Y, Cai C, Zhong C, Zhu L, Yuan M, Ren H. 2010. The type II Arabidopsis formin 14 interacts with microtubules and microfilaments to regulate cell division. *The Plant Cell* **22,** 2710–2726.

Marc J, Granger C, Brincat J, Fisher D, Kao T, McCubbin A, Cyr R. 1998. A GFP–MAP4 reporter gene for visualizing cortical microtubule rearrangements in living epidermal cells. *The Plant Cell* **10,** 1927–1939.

Martiniere A, Gayral P, Hawes C, Runions J. 2011. Building bridges: formin 1 of Arabidopsis forms a connection between the cell wall and the actin cytoskeleton. *The Plant Journal* **66,** 354–365.

Michelot A, Derivery E, Paterski-Boujemma R, Guerin C, Huang S, Parcy F, Staiger C, Blanchoin L. 2006. A novel mechanism for the formation of actin-filament bundles by a nonprocessive formin. *Current Biology* **16,** 1924–1930.

Michelot A, Guerin C, Huang S, Ingouff M, Richard S, Rodiuc N, Staiger C, Blanchoin L. 2005. The formin homology 1 domain modulates the actin nucleation and bundling activity of Arabidopsis Formin 1. *The Plant Cell* **17,** 2296–2313.

Nishimura T, Yokota E, Wada T, Shimmen T, Okada K. 2003. An Arabidopsis ACT2 dominant-negative mutation, which disturbs F-actin polimerization, reveals its distinctive function in root development. *Plant and Cell Physiology* **44,** 1131–1140.

Peremyslov V, Prokhnevsky A, Dolja V. 2010. class XI myosins are required for development, cell expansion and F-actin organization in Arabidopsis. *The Plant Cell* **22,** 1883–1897.

Petrášek J, Schwarzerová K. 2009. Actin and microtubule cytoskeleton interactions. *Current Opinion in Plant Biology* **12,** 728–734.

Rahman A, Bannigan A, Sulaman W, Pechter P, Blancaflor E, Baskin T. 2007. Auxin, actin and growth of the Arabidopsis thaliana primary root. *The Plant Journal* **50,** 514–528.

Rizvi S, Neidt E, Cui J, Feiger Z, Skau C, Gardel M, Kozmin S, Kovar D. 2009. Identification and characterization of a small molecule inhibitor of formin-mediated actin assembly. *Chemistry and Biology* **16,** 1158–1168.

Sampathkumar A, Lindeboom J, Debolt S, Gutierrez R, Ehrhardt D, Ketelaar T, Persson S. 2011. Live cell imaging reveals structural associations between the actin and microtubule cytoskeleton in Arabidopsis. *The Plant Cell* **23,** 2302–2313.

Shaw S, Kamyar R, Ehrhardt D. 2003. Sustained microtubule treadmilling in Arabidopsis cortical arrays. *Science* **300,** 1715–1718.

Smertenko A, Deeks M, Hussey P. 2010. Strategies of actin reorganisation in plant cells. *Journal of Cell Science* **123,** 3019–3028.

Smith LG, Oppenheimer DG. 2005. Spatial control of cell expansion by the plant cytoskeleton. *Annual Review of Cell and Developmental Biology* **21,** 271–295.

Sparkes I, Graumann K, Martiniere A, Schoberer J, Wang P, Osterrieder A. 2011. Bleach it, switch it, bounce it, pull it: using laser to reveal plant cell dynamics. *Journal of Experimental Botany* **62,** 1–7.

Staiger C, Sheahan M, Khurana P, Wang X, McCurdy D, Blanchoin L. 2009. Actin filament dynamics are dominated by rapid growth and severing activity in the Arabidopsis cortical array. *Journal of Cell Biology* **182,** 269–280.

Szklarczyk D, Franceschini A, Kuhn M, *et al.* 2011. The STRING database in 2011: functional interaction networks of proteins, globally integrated and scored. *Nucleic Acids Research* **39,** D561–D568.

Thitamadee S, Tuchihara K, Hashimoto T. 2002. Microtubule basis for left-handed helical growth in Arabidopsis. *Nature* **417,** 193–196.

van der Honing H, Kieft H, Emons A, Ketelaar T. 2012. Arabidopsis VILLIN2 and VILLIN3 are required for the generation of thick actin filament bundles and for directional organ growth. *Plant Physiology* **58,** 1426–1438.

Vizcay-Barrena G, Webb S, Martin-Fernandez M, Wilson Z. 2011. Subcellular and single-molecule imaging of plant fluorescent proteins using total internal reflection fluorescent microscopy (TIRFM). *Journal of Experimental Botany* **62,** 5419–5428.

Wan Y, Ash W, Fan L, Hao H, Kim M, Lin J. 2011. Variable-angle total internal reflection fluorescence microscopy of intact cells of Arabidopsis thaliana. *Plant Methods* **7,** 27.

Wang J, Xue X, Ren H. 2012. New insights into the role of plant formins: regulating the organization of the actin and microtubule cytoskeleton. *Protoplasma* **249** Suppl. 2, S101–S107.

Xue X, Guo C, Du F, Lu Q, Zhang C, Ren H. 2011. AtFH8 is involved in root development under effect of low-dose latrunculin B in dividing cells. *Molecular Plant* **4,** 264–278.

Yang W, Ren S, Zhang X, *et al.* 2011. BENT UPPERMOST INTERNODE1 encodes the class II Formin FH5 crucial for actin organization and rice development. *The Plant Cell* **23,** 661–680.

Ye J, Zheng Y, Yan A, Chen N, Wang Z, Huang S, Yang Z. 2009. Arabidopsis Formin3 directs the formation of actin cables and polarized growth in pollen tubes. *The Plant Cell* **21,** 3868–3884.

Yi K, Guo C, Chen D, Zhao B, Yang B, Ren H. 2005. Cloning and functional characterization of a formin-like protein (AtFH8) from Arabidopsis. *Plant Physiology* **138,** 1071–1082.

Zhang Y, He J, McCormick S. 2010. Interdependence of endomembrane trafficking and actin dynamics during polarized growth of arabidopsis pollen tubes. *Plant Physiology* **152,** 2200–2210.

Zhang Z, Zhang Y, Tan H, Wan Y, Li G, Liang W, Yuan Z, Hu J, Ren H, Zhang D. 2011. RICE MORPHOLOGY DETERMINANT encodes the type II formin FH5 and regulates rice morphogenesis. *The Plant Cell* **23,** 681–700.

Zimmermann P, Hirsch-Hoffmann M, Hennig L, Gruissem W. 2004. GENEVESTIGATOR. Arabidopsis microarray database and analysis toolbox. *Plant Physiology* **136,** 2621–2632.